ISMME2003-033

PARTICLE TRACKING VELOCIMETRY MEASUREMENT OF CHAOTIC MIXING IN A MICRO MIXER

Hiroaki SUZUKI
Institute of Industrial Science
The University of Tokyo
hsuzuki@iis.u-tokyo.ac.jp

Masanori NAKANO, Nobuhide KASAGI
Department of Mechanical Engineering
The University of Tokyo

Chih-Ming HO
Department of Mechanical and Aerospace Engineering
University of California, Los Angeles

Mixing of magnetic beads and bio-molecules becomes critically important in a micro-scale cell sorting system. Particle tracking velocimetry (PTV) has been employed to examine the motion of magnetic beads in a model chaotic micro-mixer. The measured trajectories of beads show good agreement with the numerical simulation previously reported [5], which has predicted the onset of chaos. The bead trajectory is reconstructed from the phase-averaged velocity field of beads to estimate the Lyapunov exponent. The optimum frequency of applied control signal exists in the range of the Strouhal number of $5 < St < 12$, which is also in accordance with the numerical simulation. The present method of estimating the Lypaunov can be used to determine the performance of the mixing device for micro particles and large molecules.

Keywords: *Chaotic Mixing, Cell Sorting, Magnetic Beads, Micro Fluidics, Bio-MEMS*

INTRODUCTION

Mixing is an important technical target in micro-fluidic systems, such as μ-TAS and Lab-on-a-Chip [1]. In such a tiny scale (<1mm), the flow is mostly in the creeping flow regime, so that major mixing mechanisms in macro scales (turbulence and separation) are not available. Especially, in developing a micro biological assay system, the mixing of large suspended substances (e.g., cells, proteins, DNAs) becomes much less efficient than water-soluble materials due to their small diffusivity [2].

In bio-technology, magnetic-beads (spherical polymer micro-beads containing iron-oxide) coated with ligand or antibody are used for the selective sorting of bio-molecules [3]. When added to a complex bio-molecule mixture, the coated magnetic beads specifically attach to the target molecules due to an immunological reaction. Eventually, the magnetically tagged molecules are separated by applying an external magnetic field. Its gentle nature and high-selectivity are suitable for the separation of precious samples, such as stem cells. Mixing of magnetic beads and biological suspension becomes crucial when one tries to integrate this system on a chip.

In the previous reports, we fabricated and tested a novel magnetic-bead based micro mixer using MEMS technology [4]. It was shown that the magnetic beads suspended in a micro-channel can be manipulated by a local magnetic field generated by micro-conductors. To mix magnetic beads efficiently, combination of a serpentine shaped channel and unsteady distributed magnetic fields were proposed. The chaotic feature of the motion of magnetic beads was revealed by means of 2-D numerical simulation [5].

However, there is a serious difficulty in quantifying the degree of mixing of beads or large bio-molecules experimentally. The conventional mixing index, which is derived from the distribution of concentration, is impractical, because, in a good mixer, the suspended particles are dispersed immediately and the interface is readily smeared out. Nevertheless, the continuous mixing may still be necessary to further enhance their chance of collision.

The aim of this report is to propose a new experimental diagnostic methodology to evaluate the chaotic mixing of micro particles. Two-dimensional microscopic particle tracking velocimetry (PTV) is used to track every single magnetic bead in the micro-mixer. Reconstructed trajectories of beads are analyzed and compared with the numerical simulation results.

NOMENCLATURE

x, y, z	Coordinates in streamwise, cross-stream, and wall-normal directions, respectively, μm
u, v	Velocities in streamwise and cross-stream directions, respectively, μm/s
$d\boldsymbol{x}(t)$	Distance between two elements at time t
$\boldsymbol{u}_p$	Bead velocity, μm/s
$\boldsymbol{F}_m$	Magnetic force, pN
f, T	Frequency, Hz, and period of control signal, s; $f = 1/T$
L, W, H	Length, width and height of one unit of the mixing channel, μm
V	Mean fluid velocity in the measurement plane, μm/s
Re	Reynolds number, VW/ν
St	Strouhal number of control signal, fW/V
σ	Lyapunov exponent

MAGNETIC MICRO MIXER

Basic Structure

The present magnetic micro-mixer is depicted in Fig. 1(a). It consists of micro-conductors embedded in the silicon substrate and a micro channel formed on its top. The embedded high aspect-ratio conductors, which are fabricated by deep RIE etching followed by copper electroplating, allow a relatively large current (more than 1A) to generate a magnetic field strong enough to manipulate nearby magnetic beads [4]. Two streams, i.e. bio-fluid and micro magnetic bead suspension, flow in from the respective inlets and meet together at the mixing region. Then, magnetic beads are mixed by the local and time-varying distributed magnetic fields generated by micro-conductors to facilitate the attachment of beads to bio-molecules.

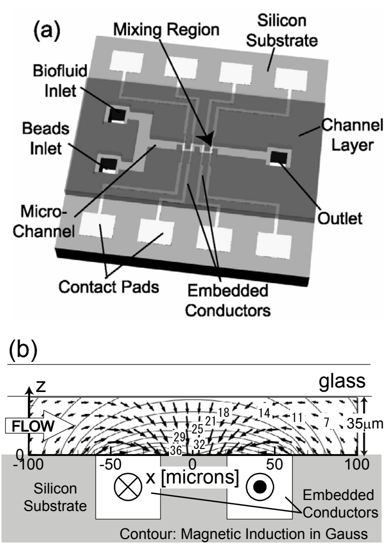

Fig 1 Conceptual diagram of the magnetic micro-mixer. (a) Perspective view. (b) Cross section of the mixing region along the channel showing induced magnetic field.

A pair of parallel current conductors is used as a basic unit of magnetic field source: when an electric current is applied in opposite directions, a magnetic field is generated in a way that magnetic beads are attracted toward them. Figure 1(b) shows the magnetic field generated by two current carrying conductors ($40\times40\mu m^2$ in the section, 40μm apart), computed based on the Bio-Savart law. Applied current is 0.5A each. A magnetic field of 30~40 gauss is generated near the center of two conductors.

Mixing Strategy

We utilize the concept of chaotic mixing in designing the shape of the channel, electrodes, and control signal. Chaotic mixing is recognized, even in a creeping flow, when the Lagrangian trajectory has a sensitive dependence on the initial condition [6]. In such a system, the distance between two initially nearby trajectories diverge exponentially fast, and the resultant state becomes unpredictable. It is known that even a two-dimensional laminar flow can be chaotic when the time-dependency is added as another dimension. Stretching and folding of material element is an important manifestation of chaos that gives rise to an exponential growth of the interface.

In open flows (e.g., a channel flow), chaotic advection can be achieved by pushing and pulling the element between the main flow (high velocity region) and the side channels/cavities (low velocity region) [7, 8]. With a magnetic force, however, only an attractive force can be induced on beads. Changing the direction of applied current simply results in the opposite polarization of a bead, so they are always attracted toward the conductors. If the same strategy is used, magnetic beads pulled into the low velocity region cannot come back to the high velocity region, and the global mixing will not be accomplished.

In the previous reports, we demonstrated that the chaotic motion of magnetic beads can be achieved with a two-dimensional serpentine channel and phase shift signal [4, 5]. Figure 2 illustrates one unit of 2-D serpentine channel, which repeats in the x direction, with four transverse conductors shown as shaded areas. The chaotic motion of magnetic beads is induced when a time-dependent control signal (phase shift signal) shown in Fig. 3 is applied. For instance, when an electric current is applied to electrodes 3 and 4 (corresponds to phase (iv)), magnetic beads flowing near the center streamline are attracted toward the low velocity region at the corner (arrow 1 in Fig. 2). At the other phase, e.g., phase (iii), the current is applied to electrodes 2 and 3, and thus beads that had been drawn into the corner are pulled back to the main stream (arrow 2). Attractive and repulsive forces can be produced by shifting the pair of working electrodes. Normalized signal frequency is defined as the Strouhal number $St = fW/V$.

PRELIMINARY FLOW VISUALIZATION

Figure 4 shows a serpentine-shaped magnetic micro-mixer fabricated. Four mixing units are repeated in the mixing region. The unit length L, width W, and height H of the channel are 320, 160, and 35 μm, respectively. The width and spacing of conductors are both 40 μm. Deionized water is flowing in the upper side of the channel, while the water suspension of 1 μm magnetic beads (Spherotech, SPHERO™ CM-10) is flowing in the lower side. The flow rate is 100 nL/min, which corresponds to the Reynolds number of $Re = WV/\nu = 4.8\times10^{-2}$ (mean velocity of V = 0.3 mm/s). In Fig. 4, it is obvious that there is no mixing or stirring effect, and the interface of two streams clearly persists to the downstream.

Figure 5 shows a snapshot of mixing process when the phase shift signal is applied ($Re = 2.4\times10^{-2}$ and St = 2.0). The interface undergoes stretching and folding repeatedly (Fig. 5a). In the downstream, beads spread all over the channel and thus a well-mixed state is achieved (Fig. 5b).

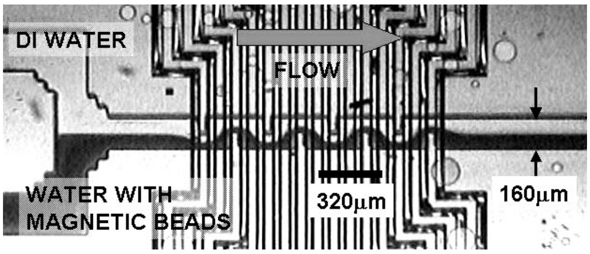

Fig. 4 Fabricated magnetic micro-mixer with a serpentine shaped channel. Magnetic beads do not mix without any disturbance.

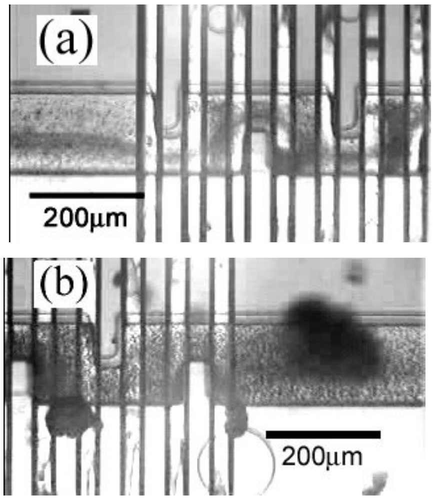

Fig. 5 (a) A snapshot of mixing process when the phase shift signal is applied. (b) Magnetic beads spread uniformly across the channel at the downstream.

PROCEDURES

Experimental Procedure of PTV Measurement

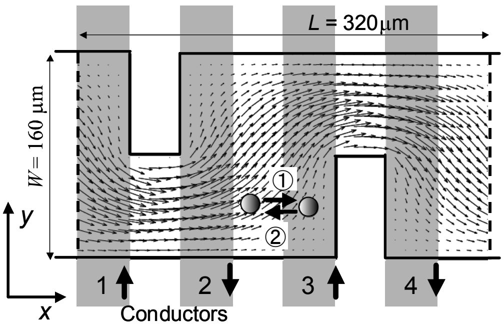

Fig. 2 Serpentine channel and transverse electrode configuration.

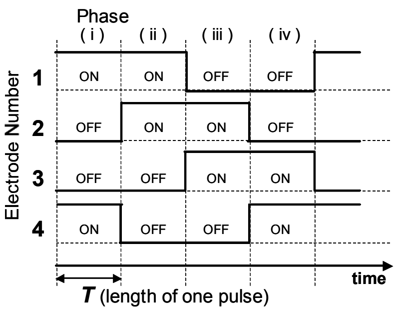

Fig. 3 Phase shift control signal. Period T is defined as the duration of one phase.

To track beads in the micro channel, the fluorescent microscopic PTV is employed. Sequential images of fluorescent magnetic beads (Spherotech, FCM-10) are captured by a NTSC CCD camera (Sony XC-7500) mounted on the microscope (Nikon E800) at 60 frame/sec, through a set of optical filters. The exposure time is set to 1/1000 s by adjusting the shutter speed. The focal depth of the microscopic system is determined by the equation proposed by Meinhart [9], and is calculated to be 7 μm in our system with ×40 magnification objective lens (NA = 0.5). In the following experiment, the image is focused at the bottom plane, so the beads captured in the images should lie in z = 0~4 μm. The acquired images are A/D converted by an image capture board (MATROX METEOR II). Instantaneous velocity vectors are obtained by tracking each particle over three consecutive time steps. A binary cross-correlation method [10] is employed to reject spurious vectors. The volume concentration of beads is 0.17%. The measurement area is 320×240 μm^2, and one pixel resolves 0.5 μm. The trajectories of magnetic beads are reconstructed from the time sequence of instantaneous velocity data in the post-processing.

Numerical Procedure

The data extracted from PTV measurement is compared with the two-dimensional numerical simulation results presented in the previous report [5]. In short, the steady velocity field in a serpentine channel is computed by a commercial CFD code (CFD Research Corp, CFD-ACE+), and the trajectories of beads are calculated by integrating the vector sum of induced velocities due to the fluidic drag and magnetic force.

RESULTS

Motion of Beads in Stationary Fluid

Figure 6 shows fluorescent images of magnetic beads in a straight channel with transverse conductors, which exist between the broken lines. There is no flow in the channel. When the current of 0.5 A is applied, magnetic beads originally dispersed in the channel (Fig. 6a) are attracted and accumulated at the inside edges of the conductors (Fig. 6b).

In Fig. 7, the *x*-component induced velocity $\boldsymbol{u}_p$ and the corresponding magnetic force $\boldsymbol{F}_m$ on a magnetic bead is plotted. Narrow lines represent the theoretical calculation [5] at some different *z* sections, and a thick line represents the bead velocity obtained from PTV measurement. The positive value represents the direction toward the center of two conductors (toward left). It is clear that the beads are attracted and accumulate at the inside edge of the conductor ($x \sim 20$ μm), where the profile crosses the horizontal axis. The experimental result lies between the theoretical value of $z = 1$ and 5μm. Thus, the measurement result is in good accordance with the theoretical prediction. The maximum velocity of 18 μm/s is derived at the outer edge of the electrode ($x \sim 60$ μm). The magnetic force is calculated from the equation of drag around a sphere, i.e., $\boldsymbol{F}_m = 3\pi\mu d_p \boldsymbol{u}_p$, and plotted on the right axis. The maximum magnetic force is 0.2 pN, with which the induced velocity is the maximum.

Motion of Beads in the Chaotic Flow

The particle tracking has been carried out on the serpentine channel flow. The flow rate is adjusted so that the magnitude of velocity in the measurement plane becomes close to the numerical simulation (V = 50~100 μm/s in the following PTV measurements, while V = 80 μm/s in the simulation.) It is extremely difficult to realize an exact flow rate on the order of nL/min in the present system; it is not repeatable even when the setting value on a syringe pump is the same. Probably the

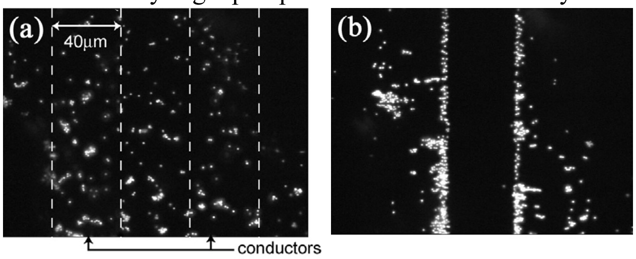

Fig. 6 Fluorescent images of magnetic beads in a straight channel. (a) Before and (b) after an electric current is applied.

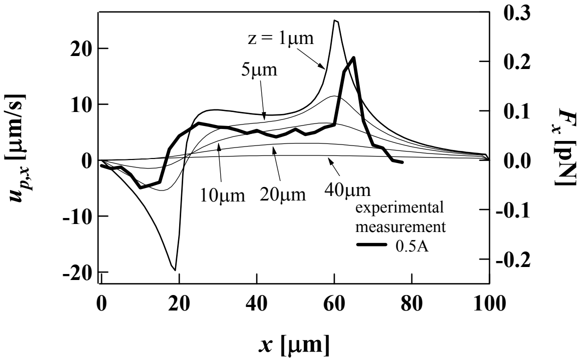

Fig. 7 *x*-component induced velocity and magnetic force on a bead in a static magnetic field.

sedimentation of beads and the trapping of even tiny air bubbles in the connecting tube affect the flow rate seriously.

Figure 8 depicts the trajectories of beads, which are tracked more than 0.3 seconds (18 frames). When no disturbance is applied, the trajectories follow the streamline of steady flow (Fig. 8a). More beads pass near the center streamline, where the flow velocity is larger, while less trajectories are obtained in the low velocity region at the corners. When the phase shift signal is applied, the number of trajectories at the corners is increased dramatically (in Fig. 8b, marked with four circles). It is clear that the beads flowing near the center streamline are attracted into the low velocity regions.

Particle trajectories obtained at phase (ii) (when the conductors 1 and 2 are turned on) are plotted in Fig. 9. The particles flowing near the outer edge of the second conductor ($x \sim 150$ μm) is going upward and slightly left (marked with an oval) by the effect of magnetic force. This observation also confirms that beads are attracted toward the corner. The movement of beads toward the corners is a major cause of the stretching and folding. Refer to [5] for more detailed discussion of the mixing process.

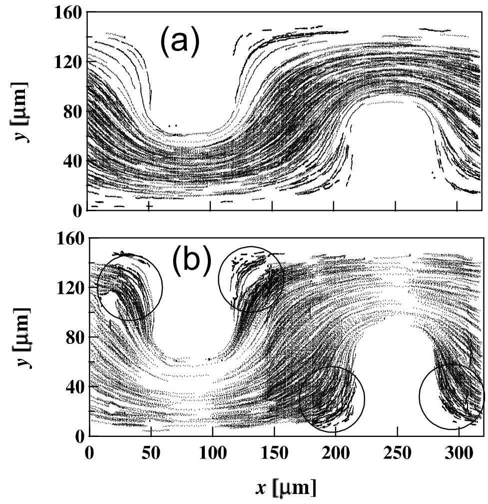

Fig. 8 Trajectories of magnetic beads which are tracked more than 0.3 seconds. (a) No magnetic force and (b) with phase shift signal.

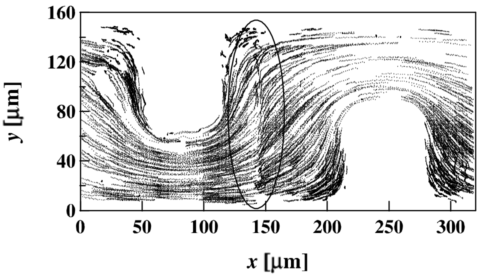

Fig. 9 Trajectories of magnetic beads when the conductor 1 and 2 are turned on.

The ensemble average of particle velocity at each control phase is taken and compared with the corresponding numerical results in Fig. 10, where working conductors are shown as squares. At every phase, magnetic beads are attracted toward the inner edges when the current is applied. For instance, when conductors 1 and 2 are on (phase (ii)), the bead velocity is decreased at the inner edge of the left conductor, and a trough is observed at $x \sim 70$ µm in the contour. On the other hand, the bead velocity is increased at the inner edge of the right conductor ($x \sim 90$ µm). The PTV measurement data clearly shows the same tendency as the numerical prediction at all phases.

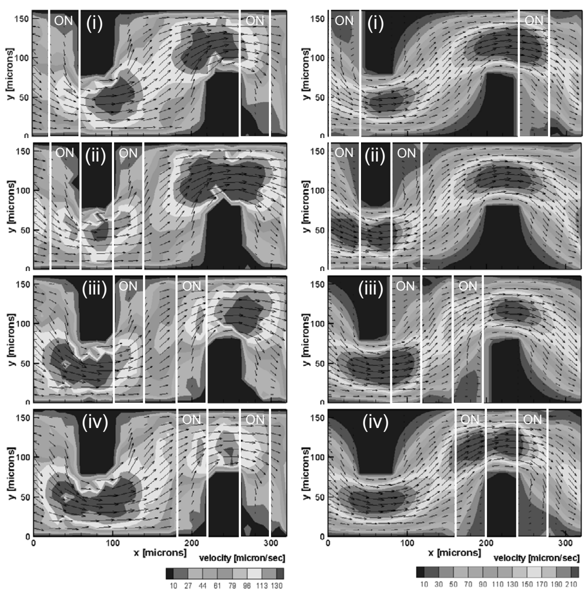

Fig. 10 Phase and spatial averages of flow velocity of magnetic beads at each control phase derived from PTV measurement (left) and numerical simulation (right).

Calculation of Lyapunov Exponent

The Lyapunov exponent (hereafter, LE) is a measure of the exponential divergence of the system, and used to quantify the degree of chaos. It is defined as

$$\sigma = \lim_{t \to \infty} \left[\frac{1}{t} \ln \left(\frac{|d\boldsymbol{x}(t)|}{|d\boldsymbol{x}(0)|} \right) \right] \tag{1}$$

where t is time, and $|d\boldsymbol{x}(0)|$ and $|d\boldsymbol{x}(t)|$ are the distance between two particles at the initial time and t, respectively. If σ is positive non-zero value, then $|d\boldsymbol{x}(t)| = |d\boldsymbol{x}(0)|\exp(\sigma t)$ and the distance of two initially nearby particles diverges exponentially with time.

In the numerical simulation, the largest LE (the largest component in the Lyapunov spectrum) is often calculated by the algorithm proposed by Wolf et al. [11], which is schematically shown in Fig. 11. Firstly, any arbitrary pair of nearby points is chosen; $|d\boldsymbol{x}(0)|$ represents their initial distance. Secondly, their new positions and distance $|d\boldsymbol{x}'(\Delta t)|$ after a certain time period Δt are calculated, and $\ln(d\boldsymbol{x}'/d\boldsymbol{x})$ is evaluated. Then, the distance between two particles are adjusted to be small enough, while the orientation is retained (Gram-Schmit Reorthonormalization, GSR). The above process is repeated and the exponent is calculated as:

$$\sigma = \lim_{n \to \infty} \frac{1}{n\Delta t} \sum \ln \left(\frac{|d\boldsymbol{x}'((n+1)\Delta t)|}{|d\boldsymbol{x}(n\Delta t)|} \right) \tag{2}$$

where n is the number of time step of GSR. The calculation of the Lyapunov exponent (stretching rate) will not be limited by the size of the system with this algorithm.

Originally, we attempted to evaluate the LE directly from the bead trajectory derived from PTV. However, it turned out difficult because, in the Wolf's method, two particles have to be tracked for a sufficiently long time so that the orientation of two particles of interest align along the most stretching direction. However, in the PTV measurement system, the consecutive tracking is limited within the field of view, and is unavoidably terminated at the end of the measurement area.

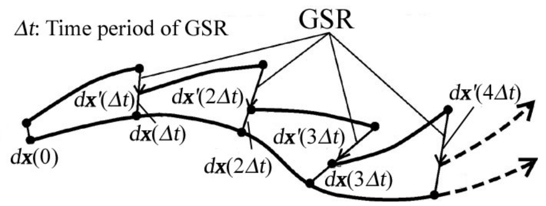

Fig. 11 Schematic of the calculation method of LE proposed by Wolf et al. [11].

Thus, an alternative indirect method for the LE calculation is necessary. Yet, we still utilize the Wolf's method; the trajectories of beads are numerically reconstructed from the phase-averaged bead velocity field, e.g., left figures in Fig. 10. The calculation procedure is as follows. From the time sequence of the instantaneous bead velocity data, ensemble average of twelve discrete time periods in one control cycle is calculated. Then, the largest LE is evaluated using the Wolf's method by numerically tracking the virtual magnetic beads flowing in the bead velocity field derived above. Time integration of bead velocity is performed using the 4-th order Runge-Kutta method.

Figure 12 shows the time convergence of the LE calculation at some different St. When no control signal is applied (steady flow), the LE converges to zero as predicted from the chaos theory. There is no exponential divergence of the initial condition. At St = 8.0, the LE converges to a constant value of 0.2. The motion of magnetic beads becomes chaotic in this frequency domain. Note that the LE in the representative chaotic systems such as Lorenz and Rossler attractors are 0.1~1.5 [11, 12]). At the control frequency larger (St = 16) and smaller (St = 4) than the chaotic regime, the LE also converges to almost zero. The global chaotic motion is suppressed at those frequencies.

Figure 13 shows the frequency dependence of the Lypaunov exponent. Circular symbols represent the LE calculated based on PTV measurement, while dotted lines show the LE calculated purely by the numerical simulation [5]. Although the profile is wider than the simulation, the exponent takes positive values at $5 < St < 13$. It indicates that the exponential divergence of the initial condition is accomplished in this driving frequency regime.

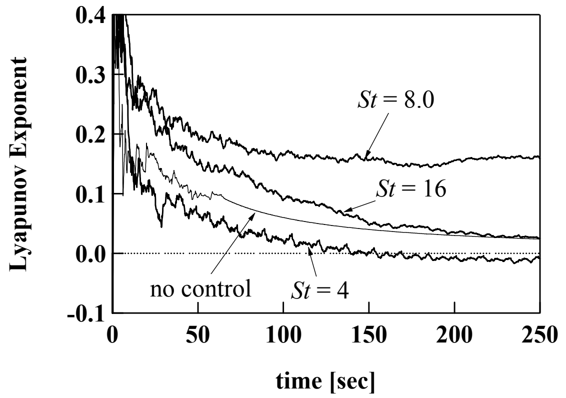

Fig. 12 Convergence of the largest Lyapunov exponent calculated from the phase-averaged data measured by PTV.

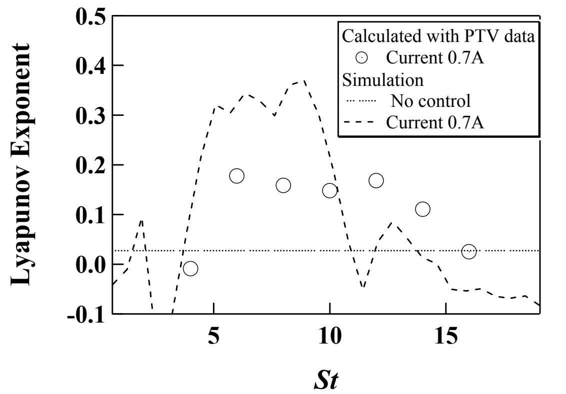

Fig. 13 Frequency dependence of the largest Lyapunov exponent.

CONCLUDING REMARKS

The motion of the magnetic beads in the chaotic micro mixer is examined by the two-dimensional fluorescent particle tracking. The bead trajectories show the motion toward the low velocity region at the corners of the serpentine shaped channel, which has been predicted to be a major cause of chaotic behavior by the numerical simulation.

As a quantitative measure of the chaotic mixing, the largest Lyapunov exponent is obtained using the phase averaged velocity field of magnetic beads. It takes positive values at $5 < St < 13$; this is also in accordance with the numerical simulation. Although the experimental determination of the Lyapunov exponent is not trivial, it is shown to be possible to approximately estimate from the reconstructed trajectories.

The algorithm of the Lyapunov exponent calculation presented in this paper can be used to quantify the performance of a mixing device for the small particles and large molecules.

ACKNOWLEDGMENTS

This work was supported through the Grant-in-Aid for Fundamental Scientific Research (S) (No. 15106004) by the Ministry of Education, Culture, Sports, Science and Technology. The authors are grateful to Professor Y. Suzuki for his help in making the PTV measurement. One of the authors (H. Suzuki) was supported by JSPS Research Fellowship for Young Scientists from 2000 to 2002. The fabrication of the device is mainly supported by DARPA/MTO.

REFERENCES

[1] Manz, A., Graber, N., and Widmer, H. M., "Miniaturized Total Chemical Analysis Systems: A Novel Concept for Chemical Sensing," Sens. Actuators B1 (1990), pp. 244-248.

[2] Ho, C. M., "Fluidics: The Link Between Micro and Nano Science and Technologies," IEEE Proc. Int. Conf. MEMS '01 (2001), pp. 375-384.

[3] Sinclair, B., "To Bead or Not to Bead: Application of Magnetic Bead Technology," The Scientist 12(13), (1998), pp. 17-20.

[4] Suzuki, H. and Ho, C. M., "A Magnetic Force Driven Chaotic Micro-Mixer," IEEE Proc. Int. Conf. MEMS '02 (2002), pp. 40-43.

[5] Suzuki, H., Kasagi, N., and Ho, C. M., "Chaotic Mixing of Magnetic Beads in Micro Cell Separator," Proc. 3rd Int. Symp. Turbulence and Shear Flow Phenomena (2003), pp. 817-822.

[6] Ottino, J. M., "The Kinematics of Mixing: Stretching, Chaos, and Transport," Cambridge University Press, 1989.

[7] Lee, Y. K., Deval, J., Tabeling, P. and Ho, C. M., "Chaotic Mixing in Electrokinetically and Pressure Driven Micro Flows," IEEE Proc. Int. Conf. MEMS '01 (2001), pp. 483-486.

[8] Deval, J., Tabeling, P. and Ho, C. M., "A Dielectrophoretic Chaotic Mixer," IEEE Proc. Int. Conf. MEMS '02 (2002), pp. 36-39.

[9] Meinhart, C. D., Wereley, S. T., and Gray, M. H. B., "Volume Illumination for Two-Dimensional Particle Image Velocimetry," Meas. Sci. Tech. 11 (2000), pp. 809-814.

[10] Yamamoto, F., Uehara, T., Iguchi, T., and Morita, Z., "A binary correlation method using a proximity function for 2-D and 3-D PTV," Exp. Numerical Flow Vis., Khalighi, B., et al., eds., New York, ASME: 23 (1991).

[11] Wolf, A., Swift, J. B., Swinney, H. L., and Vastano, J. A., "Determining Lyapunov Exponents from a Time Series," Physica 16D, pp. 285-317 (1985).

[12] Sato, S., Sano, M., and Sawada, Y., "Practical Methods of Measuring the Generalized Dimension and the Largest Lyapunov Exponent in High Dimensional Chaotic Systems," Prog. Theor. Phys., 77(1), pp. 1-5 (1987).